Throughput Performance of an Adaptive Power Splitting Relaying Protocol for Cooperative NOMA Networks

S. B. Ajibowu [1]; O. A. Adeleke[2]; O. A. Ajibola[3*]; M. O. Asafa[4]; A. A. Osobukola[5]
[1, 4, 5]Department of Electrical, Electronic, and Telecommunication Engineering, Bells University of Technology, Ota 112104, Ogun State, Nigeria
[2]Department of Electronic and Electrical Engineering, Ladoke Akintola University of Technology, Ogbomoso, Oyo State, Nigeria
[3]Department of Electrical and Electronics Engineering, Olabisi Onabanjo University, Ago-Iwoye 120107, Ogun State, Nigeria
[*]corresponding author's email: ajibola.opeyemi@oouagoiwoye.edu.ng

Abstract - *The combination of Cooperative Non-Orthogonal Multiple Access (NOMA) and Simultaneous Wireless Information and Power Transfer (SWIPT) enhances the reception reliability and communication quality of users in wireless networks. However, conventional Fixed Power Splitting (FPS) protocol limits system performance due to its inability to adapts to fluctuating channel conditions. This strategy leads to decoding errors and reduces the rate of data transmission. This paper presents an Adaptive Power Splitting (APS) NOMA protocol for two-user SWIPT-based cooperative NOMA network. The adaptive strategy enables the near user to dynamically adjust its power splitting ratio based on real-time channel conditions to optimize Energy Harvesting (EH) and Information Decoding (ID). A system model was developed by incorporating a channel-based power splitter into the near user's receiver architecture. The mathematical expressions for the Outage Probability (OP) and throughput for both users are derived over Rayleigh fading channels to evaluate the throughput performance of the proposed system. Performance analysis is conducted through MATLAB-based simulations, evaluating the effects of system parameters on the throughput performance of the considered system. The results reveal that at Signal-to-Noise-Ratio (SNR) of 25dB, APS NOMA system outperforms FPS NOMA and Orthogonal Multiple Access (OMA) by 13.33% and 29.66%, respectively, at near user, and by 4.74% and 30.38%, respectively, at the far user, validating its effectiveness for energy-constrained wireless networks and future IoT systems.*

Keywords: *cooperative communication, non-orthogonal multiple access, power splitting, simultaneous wireless information and power transfer, throughput*

Article History
Received 19 August 2025
Received in revised form 20 September 2025
Accepted 7 October 2025

I. Introduction

The increasing demand for higher data rates has led to an exponential growth of wireless communication networks. Non-Orthogonal Multiple Access (NOMA), as an advanced multiple access technique, has been identified for its potential to meet these demands. NOMA makes provision for higher spectral efficiency and supports massive device connectivity [1][2]. The merit of NOMA over OMA is that it has the capacity to enable multiple users for resources (same frequency) sharing given varying power levels simultaneously [3]. It utilizes Superposition Coding (SC) technique to combine multiple signals at the transmitter and employs Successive Interference Cancelation (SIC) to separate the combined signals at the receiver [4]. Cooperative communication, which provides spatial diversity and extends the coverage of wireless networks [5], has been integrated with NOMA to enhance the reliability of information transmission. However, cooperative NOMA nodes are mostly powered by batteries, and replacing these batteries frequently may be expensive and not practically feasible.

Simultaneous Wireless Information and Power Transfer (SWIPT) technology has been adopted for energy harvesting from Radio Frequency (RF) signals to extend the operation and lifecycle of these battery-limited devices. SWIPT employs the Time Switching (TS) and the Power Splitting (PS) protocols in wireless networks [6]. While PS involves the division of the

received signal between energy harvesting (EH) and information decoding (ID), TS switches over time between EH and ID. The amalgamation of cooperative NOMA and SWIPT is a promising solution to improve overall network efficiency.

Recently, several works have evaluated the performance of throughput in a SWIPT-integrated cooperative NOMA system. In [7], the authors investigated a SWIPT-based cooperative NOMA scheme, where spatial randomness of user locations is considered. The mathematical expression for the users was derived for the performance evaluation of the proposed system. To optimize the data rate experienced by the far users, [8] proposed an algorithm to optimize PS ratio. Results showed that the throughput of the distant user improved. Authors in [9] examined the throughput performance of the considered network, where they proposed an integrated design strategy for the power allocation (PA) coefficient and PS ratio to improve the near-user efficiency. Also, mathematical expressions for the OPs for the users are provided.

Reference [10] carried out an investigation on the throughput efficiency under delay-constrained and delay-tolerant transmission conditions. The authors provided the throughput expression for the proposed scheme. Their result showed that the performance for the PS protocol is superior to TS protocol throughout the entire signal-to-noise-ratio (SNR) region [11]. Also in [12], the performance of SWIPT NOMA network under PS protocol was investigated. The authors developed a joint scheme for optimizing PA coefficients and PS ratio to maximize data rate. Results show that the performance of Full-Duplex (FD) technique outperforms Half-Duplex (HD) when the SNR is low, while HD performs better than the FD when the SNR is high. Reference [13] evaluated the joint impact of SWIPT and cooperative NOMA over a Nakagami-m fading environment where a direct link exists. Authors derived the mathematical expression of throughput of the proposed scheme.

In the work of [14], a Decode and Forward (DF) PS protocol under two different transmission modes (delay-limited and delay-tolerant) was presented. They derived the mathematical expressions for the developed scheme with and without a direct link in terms of the performance metrics. Results confirmed that the cooperative NOMA that has direct link performs better than the system that has no direct link. However, the optimal PS ratio, needed to improve the system performance is not considered. Reference [15] presented a SWIPT-based protocol that enhances cell edge user's quality of communication. The mathematical expression is derived to evaluate the performance of TS protocol and PS protocol in the considered network.

In the work by [16], a two-user SWIPT NOMA network is examined to facilitate the operation of far users. Authors employed gradient descent technique to calculate the ideal PS ratio value that optimizes the sum throughput of the considered network. Reference [17] investigated a FD SWIPT-based cooperative NOMA access system where the near user assisted the far user via EH and FD communications. They derived the mathematical expressions of the users to evaluate the performance of the system. Their results illustrated that the proposed scheme can be employed to communicate with IoT users via EH relay.

In [18], the performance of throughput in a cooperative NOMA network using SWIPT is investigated, where the source uses a Partial Channel State Information (P-CSI) scheme to select a near user from multiple near users. The throughput expression for the proposed system is derived. Their results showed that the proposed system outperforms other user selection schemes. In the work of [19], a SWIPT-based cooperative NOMA network is examined, where the near user serves as a shared relay to assist far user to improve spectrum and energy efficiency. The mathematical expressions were derived and the impacts of SNR and power allocation on system performance were analysed through simulation.

Also, [20] developed EH-enabled cooperative NOMA network in the presence of interference. They derived the expressions for the proposed relay selection and analyse the effects of EH parameters and energy conversion efficiency on the performance of the system. Reference [21] examined the throughput performance of an EH cognitive relay scheme employing cooperative NOMA, where the source transmits combined signals to near user and cognitive users. Numerical results showed that combining relay and direct links improves the data rates of the far user. All the literatures utilized fixed PS ratio, which lacks adaptability to changing channel conditions, leading to insufficient utilization of resources and degraded throughput performance.

However, in [22], authors developed an adaptive EH to maximize capacity of dual hop network where the PS ratio changes according to instantaneous channel conditions between relay and destination. Also, [23] examined throughput performance using joint TS and PS in dual hop network. Unlike the existing adaptive schemes that primarily focused on CSI requirements, our proposed adaptive PS jointly adapts the PS ratio based on instantaneous channel conditions and target data rate of source to near user to maximize throughput while ensuring sufficient EH. The throughput mathematical expression is derived and the influences of energy conversion efficiency and PA coefficient on the throughput performance of the network are investigated.

The major contributions of this paper are given as follows:

a) An APS NOMA protocol where the near user dynamically adapts its PS ratio based on the channel conditions and target data rate is proposed to enhance energy harvesting and optimize throughput.
b) The mathematical expressions for the users to characterize the performance of the proposed APS NOMA system are derived.

c) The impact of energy conversion efficiency, distance, and power allocation on the throughput performance of the considered network is investigated.
d) Comparison of the throughput of the proposed APS scheme, the FPS scheme, and the OMA scheme.

Other sections of the paper are structured as follows: Section II introduces the system model and assumptions for the proposed adaptive relaying protocol. In Section III, the analysis of the OP is presented while Section IV provides the throughput performance analysis of the proposed scheme. Section V provides the numerical results and discussions for system performance evaluation. Lastly, Section VI gives the summary of key findings for the research.

II. System Model

This paper considered a downlink two-user SWIPT-enabled Cooperative NOMA network that consist of a Source (S), User A (U_A), and User B (U_B) as presented in Fig. 1. Each node is equipped with a single antenna and operates in HD mode. User A serves as a relay and employs DF protocol to assist source information transmission to User B. User A employs an adaptive PS receiver architecture for EH and ID. In this model, β_s portion is used for EH, while $(1-\beta_s)$ portion is used for ID, where $\beta_s(0<\beta_s<1)$ is the PS ratio. The distances from S to U_A, S to U_B, and U_A to U_B are denoted by d_1, d_0, and d_2, respectively, and the path loss exponent is denoted by m. Wireless links in the system model are independent and identically distributed and follow Rayleigh fading distribution. h_{U_A}, $h_{U_AU_B}$, and h_{U_B} represent the channel coefficient from S to U_A, U_A to U_B, and S to U_B, respectively.

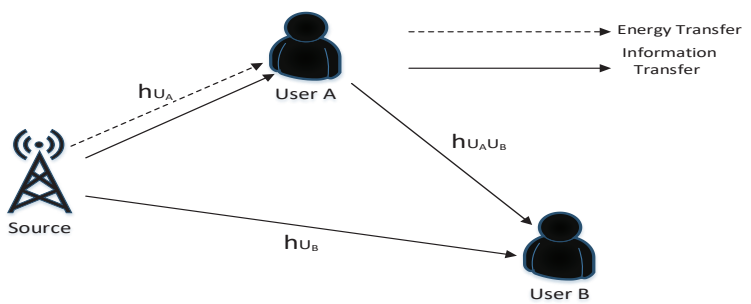

Fig. 1. System Model for the Proposed System

A. Direct Transmission and Energy harvesting of the proposed APS SWIPT-based CNOMA

During the transmission the phase, the source transmits the superposed signals, s_1 and s_2, to U_A and U_B respectively. The U_A harnesses energy from the RF signal broadcast by the source with adaptive PS ratio β_s. Therefore, the signal received at the EH receiver and U_B is expressed as

$$y_{U_A} = h_{U_A}\left(\sqrt{\frac{\beta_s P_s a_1}{d_1^m}}s_1 + \sqrt{\frac{\beta_s P_s a_2}{d_1^m}}s_2\right) + n_{U_A} \quad (1)$$

$$y_{U_B} = h_{U_B}\left(\sqrt{\frac{P_s a_1}{d_0^m}}s_1 + \sqrt{\frac{P_s a_2}{d_0^m}}s_2\right) + n_{U_B} \quad (2)$$

where P_s is the transmitting power at source S, with n_{U_A} and n_{U_B} representing the Additive White Gaussian Noise (AWGN) at U_A and U_B respectively.

The harvested energy at U_A can be expressed as

$$E_H = \frac{\beta_s \eta |h_{U_A}|^2 P_s (T/2)}{d_1^m} \quad (3)$$

where η is the energy conversion efficiency

$\beta_s = \frac{(2^{2R_1}-1)\sigma_1^2 d_1^m}{P_s|h_{U_A}|^2}$, which is a function of channel gain between S and U_A.

The transmitted power at U_A is expressed as

$$P_R = \frac{E_H}{T/2} \quad (4)$$

Substituting the value of E_H in (3) into (4), the transmitted power from U_A becomes

$$P_R = \frac{\beta_s \eta P_S |h_{U_A}|^2}{d_1^m} \quad (5)$$

B. Information Processing and Cooperative Transmission

On the other hand, the RF signal at the information receiver of U_A in the APS scheme is given by

$$y_{IR} = h_{U_A} + \left(\sqrt{\frac{(1-\beta_s)P_s a_1}{d_1^m}}s_1 + \sqrt{\frac{(1-\beta_s)P_s a_2}{d_1^m}}s_2\right) + n_{U_A} \quad (6)$$

According to the NOMA principle, U_A first decodes U_B message by treating its message as interference, then removes s_2 symbol, and finally decodes its message. Therefore, the signal-to-Interference plus Noise Ratio

(SINR) necessary for U_A to decode the s_2 symbol is given by

$$\gamma_{SU_A}^{s_2} = \frac{(1-\beta_S)\left|h_{U_A}\right|^2 a_2 P_S}{(1-\beta_S)\left|h_{U_A}\right|^2 a_1 P_S + d_1^m \sigma_1^2} \quad (7)$$

After the utilization of SIC at U_A, where all interference is cancelled out from the received signal, the received SNR for U_A to decode its own signal s_1 is expressed as

$$\gamma_{SU_A}^{s_1} = \frac{(1-\beta_S)P_S\left|h_{U_A}\right|^2 a_1}{(1-\beta_S)P_S\left|h_{U_A}\right|^2 a_2 + d_1^m \sigma_1^2} \quad (8)$$

similarly, the received SINR at U_B to decode s_2 directly from S is given by

$$\gamma_{SU_B}^{s_2} = \frac{P_S\left|h_{U_B}\right|^2 a_2}{P_S\left|h_{U_B}\right|^2 a_1 + d_0^m \sigma_0^2} \quad (9)$$

meanwhile, the decoded signal s_2 at U_A is sent to U_B. The signal received at U_B is expressed as

$$y_{U_A U_B} = h_{U_A U_B}\left(\sqrt{\frac{P_R}{d_1^m}} s_2\right) + n_{U_B} \quad (10)$$

substituting equation (5) into (10), $y_{U_A U_B}$ becomes

$$y_{U_A U_B} = \left(\sqrt{\frac{\beta_S \eta P_S \left|h_{U_A}\right|^2}{d_1^m d_2^m}} s_2\right) h_{U_A U_B} + n_{U_B} \quad (11)$$

The received SNR at far user via the relaying path is given by

$$y_{U_A U_B} = \left|h_{U_A U_B}\right|^2 \left|h_{U_A}\right|^2 \xi P_S \quad (12)$$

where $\xi = \frac{\beta_S \eta}{d_1^m d_2^m}$ is the EH factor which captures the impact of APS ratio β_s, energy conversion efficiency η, distances d_1 and d_2, and the path loss exponent m.

U_B receives information from both the relaying and direct paths, and combines these using Maximal Ratio Combining (MRC) to improve reception reliability. The combined SINR is given as

$$\gamma_{U_B}^{MRC} = \left|h_{U_A U_B}\right|^2 \left|h_{U_A}\right|^2 \xi P_S + \frac{P_S\left|h_{U_B}\right|^2 a_2}{P_S\left|h_{U_B}\right|^2 a_1 + d_0^m \sigma_0^2} \quad (13)$$

III. System Model

A. Outage Probability of the Near User

User U_A will not suffer an outage if both signals s_1 and s_2 received from the S can be successfully decoded. Thus, the OP of U_A can be expressed as $P_{out}^N = 1 - P_r(\gamma_{SU_A}^{s_2} > \gamma_{th2}, \gamma_{SU_A}^{s_1} > \gamma_{th1})$ (14)

where, $\gamma_{th1} = 2^{2R_1} - 1$ and $\gamma_{th2} = 2^{2R_2} - 1$ are the threshold SNRs for correctly decoding information s_1 and s_2, respectively.

Substituting equations (7) and (8) into equation (14), the outage probability at U_A yields

$$P_{out}^N = 1 - P_r\left(\frac{(1-\beta_S)P_S\left|h_{U_A}\right|^2 a_2}{(1-\beta_S)P_S\left|h_{U_A}\right|^2 a_1 + d_1^m \sigma_1^2} > \gamma_{th2}, \frac{(1-\beta_S)P_S\left|h_{U_A}\right|^2 a_1}{(1-\beta_S)P_S\left|h_{U_A}\right|^2 a_2 + d_1^m \sigma_1^2} > \gamma_{th1}\right) \quad (15)$$

Solving the equation (15) gives

$$P_{out}^N = 1 - P_r\left(\left|h_{U_A}\right|^2 > \frac{\gamma_{th_2} d_1^m \sigma_1^2}{(1-\beta_S)P_S(a_2 - a_1\gamma_{th_2})}, \left|h_{U_A}\right|^2 > \frac{\gamma_{th_1} d_1^m \sigma_1^2}{(1-\beta_S)P_S(a_1 - a_2\gamma_{th_1})}\right) \quad (16)$$

$$P_{out}^N = 1 - P_r\left(\left|h_{U_A}\right|^2 > \frac{\gamma_{th_2} d_1^m \sigma_1^2}{(1-\beta_S)P_S(a_2 - a_1\gamma_{th_2})}\right) P_r\left(\left|h_{U_A}\right|^2 > \frac{\gamma_{th_2} d_1^m \sigma_1^2}{(1-\beta_S)P_S(a_1 - a_2\gamma_{th_1})}\right) \quad (17)$$

$$P_{out}^N = 1 - Q_1 Q_2 \quad (18)$$

where,

$$Q_1 = P_r\left(\left|h_{U_A}\right|^2 > \frac{\gamma_{th_2} d_1^m \sigma_1^2}{(1-\beta_S)P_S(a_2 - a_1\gamma_{th_2})}\right) \text{ and}$$

$$Q_2 = P_r\left(\left|h_{U_A}\right|^2 > \frac{\gamma_{th_2} d_1^m \sigma_1^2}{(1-\beta_S)P_S(a_1 - a_2\gamma_{th_1})}\right)$$

Solving the first term Q_1 in equation (17) becomes $Q_1 = \int_{\frac{\gamma_{th_2} d_1^m \sigma_1^2}{(1-\beta_S)P_S(a_2 - a_1\gamma_{th_2})}}^{\infty} f_{\left|h_{U_A}\right|^2}(y)\, dy =$

$$\exp\left(-\frac{\gamma_{th_2} d_1^m \sigma_1^2}{(1-\beta_S)P_S(a_2 - a_1\gamma_{th_2})}\right) \quad (19)$$

Solving the second term Q_2 also becomes

$$Q_2 = \int_{\frac{\gamma_{th_1} d_1^m \sigma_1^2}{(1-\beta_S)P_S(a_1 - a_2\gamma_{th_1})}}^{\infty} f_{\left|h_{U_A}\right|^2}(y)\, dy =$$

$$\exp\left(-\frac{\gamma_{th_1} d_1^m \sigma_1^2}{(1-\beta_S)P_S(a_1 - a_2\gamma_{th})}\right) \quad (20)$$

Substituting equations (19) and (20) into (18) gives

$$P_{out}^N = 1 - \left[\exp\left(-\frac{\gamma_{th_2} d_1^m \sigma_1^2}{(1-\beta_S)P_S(a_2 - a_1\gamma_{th_2})} + \frac{\gamma_{th_1} d_1^m \sigma_1^2}{(1-\beta_S)P_S(a_1 - a_2\gamma_{th_1})}\right)\right] \quad (21)$$

Therefore, the mathematical expression of OP at U_A for the developed system is given as

$$P_{out}^N = 1 - \exp\left[-\frac{d_1^m \sigma_1^2}{P_S}\left(\frac{\gamma_{th_2}}{(1-\beta_S)(a_2 - a_1\gamma_{th_2})} + \frac{\gamma_{th_1}}{(1-\beta_S)(a_1 - a_2\gamma_{th_1})}\right)\right] \quad (22)$$

B. Outage Probability of the Far User

User U_B avoids outage, provided that s_2 is correctly decoded at User U_A and also at User U_B. Thus, the OP experienced by User U_B is expressed as

$$P_{out}^F = P_r(\gamma_{SU_A}^{s_2} < \gamma_{th2}, \gamma_{SU_B}^{s_2} < \gamma_{th2}) + P_r(\gamma_{SU_A}^{s_2} \geq \gamma_{th2}, \gamma_{U_B}^{MRC} < \gamma_{th2}) \quad (23)$$

Substituting equations (7), (9) and (13) into (23) yields

$$P_{out}^{F} = P_r\left(\frac{(1-\beta_s)P_s\left|h_{U_A}\right|^2 a_2}{(1-\beta_s)P_s\left|h_{U_A}\right|^2 a_1 + d_1^m\sigma_1^2} < \gamma_{th2}, \frac{P_s\left|h_{U_B}\right|^2 a_2}{P_s\left|h_{U_B}\right|^2 a_1 + d_0^m\sigma_0^2} < \gamma_{th2,}\right) + P_r\left(\frac{(1-\beta_s)P_s\left|h_{U_A}\right|^2 a_2}{(1-\beta_s)P_s\left|h_{U_A}\right|^2 a_1 + d_1^m\sigma_1^2} \left|h_{U_A}\right|^2 \xi P_s + \frac{P_s\left|h_{U_B}\right|^2 a_2}{P_s\left|h_{U_B}\right|^2 a_1 + d_0^m\sigma_0^2}\right) \quad (24)$$

Solving the equation (24) gives

$$P_{out}^{F} = P_r\left(\left|h_{U_A}\right|^2 > \frac{\gamma_{th_2} d_1^m \sigma_1^2}{(1-\beta_s)\,P_s(a_2 - a_1\gamma_{th_2})}, \left|h_{U_B}\right|^2 > \frac{\gamma_{th_2} d_0^m \sigma_0^2}{P_s(a_2 - a_1\gamma_{th_2})}\right) +$$

$$P_r\left(\left|h_{U_A}\right|^2 > \frac{\gamma_{th_2} d_1^m \sigma_1^2}{(1-\beta_s)\,P_s(a_2 - a_1\gamma_{th_2})}, /h_{U_A U_B}/^2 < \frac{\gamma_{th_2} d_2^m \sigma_2^2}{\left|h_{U_A}\right|^2 \xi P_s}, \left|h_{U_B}\right|^2 < \frac{\gamma_{th_2} d_0^m \sigma_0^2}{P_s(a_2 - a_1\gamma_{th_2})}\right) \quad (25)$$

$$P_{out}^{F} = Q_1 Q_3 + Q_1 Q_4 Q_3 \quad (26)$$

The Q_3 term can be solved by applying equation (1) and (2) to become

$$Q_3 = \int_{\frac{\gamma_{th_2} d_0^m \sigma_0^2}{P_s(a_2 - a_1\gamma_{th_2})}}^{\infty} f_{/h_{U_B}/^2}(y)\, dy = \exp\left(-\frac{\gamma_{th_2} d_0^m \sigma_0^2}{P_s(a_2 - a_1\gamma_{th_2})}\right) \quad (27)$$

Solving the term Q_4 also becomes

$$Q_4 = \int_{\frac{\gamma_{th_2} d_2^m \sigma_2^2}{\xi P_s}}^{\infty} f_{/h_{U_A U_B}/^2}(y)\, dy = \exp\left(-\frac{\gamma_{th_2} d_2^m \sigma_2^2}{\xi P_s}\right) \quad (28)$$

Substitute equation (19), (27) and (28) into (26) yields

$$P_{out}^{F} = \exp\left(-\frac{\gamma_{th_2} d_1^m \sigma_1^2}{(1-\beta_s)\,P_s(a_2 - a_1\gamma_{th_2})}\right) + \exp\left(-\frac{\gamma_{th_2} d_0^m \sigma_0^2}{P_s(a_2 - a_1\gamma_{th_2})}\right) + \exp\left(-\frac{\gamma_{th_2} d_1^m \sigma_1^2}{(1-\beta_s)\,P_s(a_2 - a_1\gamma_{th_2})}\right) + \exp\left(-\frac{\gamma_{th_2} d_2^m \sigma_2^2}{\xi P_s}\right) + \exp\left(-\frac{\gamma_{th_2} d_0^m \sigma_0^2}{P_s(a_2 - a_1\gamma_{th_2})}\right) \quad (29)$$

$$P_{out}^{F} = \exp\left[-\frac{\gamma_{th_2}}{P_s}\left(\frac{d_1^m \sigma_1^2}{(1-\beta_s)(a_2 - a_1\gamma_{th_2})} + \frac{d_0^m \sigma_0^2}{(a_2 - a_1\gamma_{th_2})} + \frac{d_1^m \sigma_1^2}{(1-\beta_s)\,(a_2 - a_1\gamma_{th_2})} + \frac{d_2^m \sigma_2^2}{\xi P_s} + \frac{d_0^m \sigma_0^2}{(a_2 - a_1\gamma_{th_2})}\right)\right] \quad (30)$$

Therefore, the mathematical expression of OP at U_B for the developed system is given as

$$P_{out}^{F} = \exp\left[-\frac{\gamma_{th_2}}{P_s}.2\left(\frac{d_1^m \sigma_1^2}{(1-\beta_s)(a_2 - a_1\gamma_{th_2})} + \frac{d_0^m \sigma_0^2}{(a_2 - a_1\gamma_{th_2})} + \frac{d_2^m \sigma_2^2}{2\xi P_s}\right)\right] \quad (31)$$

IV. Throughput Performance Analysis

This section provides the throughput expression of the proposed APS NOMA protocol, which is derived based on the OP expressions to evaluate system performance. The throughput of the network is defined by the aggregate data correctly received at U_B and U_A. The throughput of the proposed system can be expressed as

$T_{total} = (1\text{-}P_{out}^{F})R_1 + (1\text{-}P_{out}^{N})R_2$ (32)

where, P_{out}^{N} and P_{out}^{F} are the expressions derived for OP at U_A and U_B, which are expressed in equations (22) and (31) respectively.

Substituting (31) and (22) into (32), the expression of the total system throughput for the considered system is given by

$$T_{total} = \left\{1 - \exp\left[-\frac{\gamma_{th_2}}{P_s}.2\left(\frac{d_1^m \sigma_1^2}{(1-\beta_s)(a_2 - a_1\gamma_{th_2})} + \frac{d_0^m \sigma_0^2}{(a_2 - a_1\gamma_{th_2})} + \frac{d_2^m \sigma_2^2}{2\xi P_s}\right)\right]\right\} R_1 + \left\{1 - \exp\left[-\frac{d_0^m \sigma_0^2}{P_s}\left(\frac{\gamma_{th_2}}{(1-\beta_s)(a_2 - a_1\gamma_{th_2})} + \frac{\gamma_{th_1}}{(1-\beta_s)(a_1 - a_2\gamma_{th_1})}\right)\right]\right\} R_2 \quad (33)$$

This expression captures the effects of power allocation coefficients, energy conversion efficiency, and distance from the source to the near user.

V. Results and Discussion

The results to compare the performance of throughput for the developed APS NOMA, FPS NOMA, and OMA schemes are presented in this section. In the simulation, which was carried out in a MATLAB environment, PA ratios are set as $a_1 = 0.2$ and $a_2 = 0.8$ for U_A and U_B, respectively. Energy conversion efficiency $\eta = 0.8$, path loss exponent $m = 3$, and target data rates for U_A, $R_1 = 1.5$ bits/s/Hz and $R_2 = 1.0$ bits/s/Hz for U_B. Table 1 shows the description of important notations.

TABLE I
LIST OF NOTATIONS

Notation	Description
$\mathbf{P_s}$	Transmission power at S
$\mathbf{P_R}$	Transmission power at U_A
$\mathbf{a_1}$	Power allocation ratio for U_A
$\mathbf{a_2}$	Power allocation ratio for U_B
$\mathbf{h_{U_A}}$	Channel coefficient of S-U_A
$\mathbf{h_{U_B}}$	Channel coefficient of S-U_B
$\mathbf{h_{U_AU_B}}$	Channel coefficient of U_A-U_B
$\mathbf{\lvert h_{U_A}\rvert^2}$	Channel gain of S-U_A
$\mathbf{\lvert h_{U_B}\rvert^2}$	Channel gain of S-U_B
$\mathbf{\lvert h_{U_AU_B}\rvert^2}$	Channel gain of U_A-U_B
$\mathbf{n_{U_A}}$	Additive White Gaussian Noise at n_{U_A}
$\mathbf{n_{U_B}}$	Additive White Gaussian Noise at n_{U_B}
$\boldsymbol{\gamma_{th_1}}$	SNR threshold of U_A
$\boldsymbol{\gamma_{th_2}}$	SNR threshold of U_B
$\mathbf{R_1}$	Target data rate of U_A
$\mathbf{R_2}$	Target data rate of U_B
$\boldsymbol{\eta}$	Energy conversion efficiency
$\mathbf{m}$	Path loss exponent
$\boldsymbol{\beta_s}$	Adaptive PS ratio
$\mathbf{d_1}$	Distance from S-U_A
$\mathbf{d_0}$	Distance from S-U_B
$\mathbf{d_2}$	Distance from U_A-U_B

Fig. 2 depicts the graph of throughput of U_A and U_B as a function of transmit SNR for APS NOMA, FPS NOMA, and OMA schemes. At a SNR of 25 dB, APS NOMA for near user achieves the throughput of 4.83 bits/s/Hz, compared to 4.26 bits/s/Hz for FPS NOMA and 3.73 bits/s/Hz for OMA, indicating that APS NOMA outperforms FPS NOMA by 13.33% and OMA by 29.66%. Also at SNR of 25dB, APS NOMA of far user achieves the throughput of 2.95 bits/s/Hz, compared to 2.82 bits/s/Hz for FPS NOMA and 2.27 bits/s/Hz for OMA, indicating that APS NOMA outperforms FPS NOMA by 4.74% and OMA by 30.38%.

It is observed that the throughput of the users for the three schemes increases as SNR increases, indicating improved reliability. Also, U_A has a better performance than U_B for APS NOMA and FPS NOMA schemes. It is also shown from the graph that the APS NOMA scheme consistently performs better than the FPS NOMA and OMA schemes for both users by achieving the highest throughput across the entire SNR range. However, OMA has sub-optimal performance due to its inherently lower spectral efficiency.

The influence of η on the throughput performance of the proposed APS NOMA scheme is illustrated in Fig, 3. It is evident that the throughput performance of APS NOMA and OMA schemes for both users increases as η increases. APS NOMA outperforms both the FPS NOMA and OMA schemes, indicating its efficiency in leveraging energy harvested. Also, there is a slight improvement in FPS NOMA with η, but it remains lower than APS NOMA. However, OMA maintains a constant and lower throughput, not affected by η, owing to its fixed and less efficient resource allocation strategy.

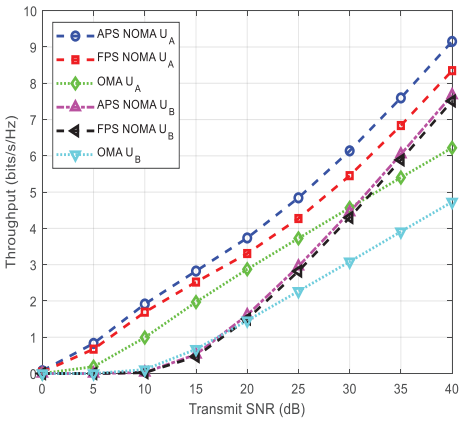

Fig. 2. Throughput Performance against Transmit SNR

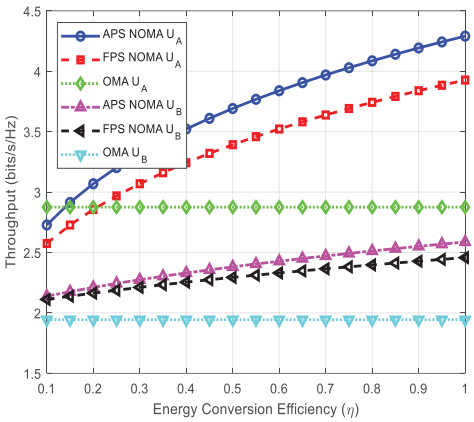

Fig. 3. Throughput Performance against Energy Conversion Efficiency

Fig. 4 shows the relationship between the throughput and distance from the source to near user d_1, of the proposed system. It can be observed from the graph that, as d_1 increases, the throughput performance of U_A decreases across all schemes due to a weak channel condition that weakens the quality of the received signal and larger path loss. However, there is a difference in the rate at which these schemes decline. OMA scheme experiences the most severe drop, FPS NOMA exhibits gradual degradation, while APS NOMA shows the highest resilience owing to adaptive power control. At U_B, the throughput remains relatively constant across all schemes, with APS NOMA achieving slightly better performance due to the ability of U_A to harvest more energy and efficiently transmit data using adaptive control.

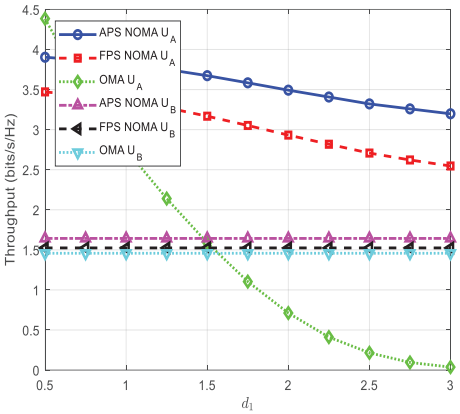

Fig. 4. Throughput Performance against Distance from Source to Near User

Fig. 5 depicts the throughput performance against β. Throughput decreases when the values of β are low and high. When β is low, less power is allocated to EH. As a result, the probability of successful decoding at U_B is lowered. Similarly, when β is high, the likelihood of correct message decoding at U_A reduces. There exists an optimal β that maximizes the throughput. At U_A, APS NOMA achieves a maximum throughput of 2.55 bits/s/Hz at β = 0.6, while FPS NOMA achieves maximum throughput at 2.48 bits/s/Hz. OMA experienced the lowest maximum throughput, around 1.20 bits/s/Hz. At U_B, APS NOMA attains the highest achievable throughput of 2.10 bits/s/Hz, while FPS NOMA attains the highest achievable throughput of 1.84 bits/s/Hz. OMA experienced the lowest maximum throughput, around 0.78 bits/s/Hz.

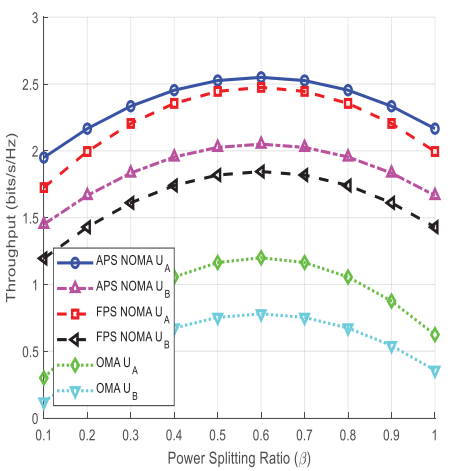

Fig. 5. Throughput Performance against Power Splitting Ratio

As shown in the Fig., APS NOMA achieves the highest throughput performance for the users, performing better than FPS NOMA and OMA schemes across the entire range of β. This performance gain is due to its dynamic ability to adjust β based on instantaneous channel condition to ensure optimal balance between EH and ID. However, these gains come with a potential trade-off between performance and complexity. While APS NOMA offers superior throughput, it requires accurate and frequent CSI acquisition, which increases system complexity.

Fig. 6 shows the graph of throughput of U_A and U_B against PA ratio a, for APS NOMA, FPS NOMA, and OMA schemes. It can be seen from the graph that, as the value of a increases, the throughput of the U_A initially increases due to better SIC decoding performance and reaches a maximum peak at a = 0.6, after which it begins to degrade as more power is shifted away. APS NOMA achieves a maximum throughput of 2.10 bits/s/Hz at a = 0.6, outperforming FPS NOMA at 1.80 bits/s/Hz and OMA at 1.65 bits/s/Hz.

At U_B, throughput steadily increases with, a as more power is allocated to them, but also peaks around 0.5 - 0.7 and then declines due to diminishing returns. APS NOMA achieves a maximum throughput of 1.40 bits/s/Hz, compared to 1.20 bits/s/Hz for FPS NOMA and 1.10 bits/s/Hz for OMA. The APS NOMA consistently performs better than FPS NOMA and OMA for both users, achieving the highest throughput performance across all values of a owing to its adaptive ability to adjust power based on channel conditions. OMA shows the lowest throughput across all values of a due to orthogonal division of resources.

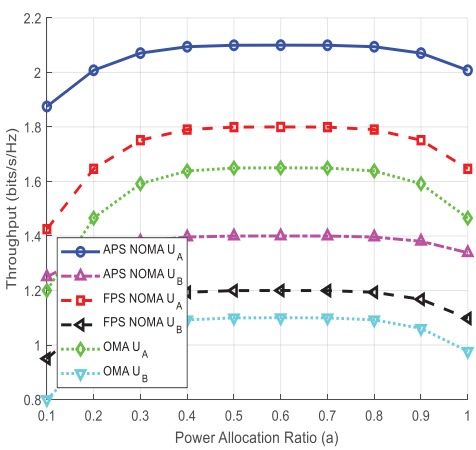

Fig. 6. Throughput Performance against Power Allocation Ratio

VI. Conclusion

This paper presents performance analysis of throughput in a cooperative NOMA network using APS protocol. This strategy adjusts the PS ratio based on real-time channel conditions and target data rate, thereby enhancing EH and ID capabilities of the near user. The mathematical expressions for the OP and throughput of both users for the proposed system over Rayleigh fading channel were derived. We also analysed the throughput performance of the proposed APS NOMA scheme. The results revealed that the proposed APS NOMA outperforms both the FPS NOMA and OMA schemes in terms of throughput, highlighting its importance in balancing EH and ID, leading to improved throughput performance. Future research will explore deep reinforcement learning for real-time power allocation in dynamic network environments.

Conflict of Interest

The authors declare no conflict of interest in the publication process of the research article.

Author Contributions

Author 1: Conceptualization, analysis, result interpretation, writing–original draft preparation, review; Author 2: Supervision, draft review and editing, investigation; Author 3: Editing, investigation, review; Author 4: Review, editing; Author 5: Review, editing.

References

[1] Z. Ding, X. Lei, G.K. Karagiannidis, R. Schober, J. Yuan, and V.K. Bhargava, "A Survey on Non-Orthogonal Multiple Access for 5G networks: Research Challenges and Future Trends," *IEEE J. Sel. Areas Commun.,* vol. 35, no. 10, pp. 2181-2195, 2017.

[2] L. Dai, B. Wang, Y. Yuan, S. Han, I. Chih-Lin, and Z. Wang, "Non-Orthogonal Multiple Access for 5G solutions, Challenges, opportunities and future research trends," *IEEE Commun*, vol. 53, no. 9, pp. 74-81, 2015.

[3] Y. Saito, A. Benjebbour, Y. Kishiyama, and T. Nakamura, "System-Level Performance Evaluation of Downlink Non-Orthogonal Multiple Access", 2013 *IEEE 24th Annual International Symposium on Personal, Indoor, and Mobile Radio Communications*, pp. 611-615, 2013.

[4] M. Aldababsa, and E. Basar, "Joint Transmit and Receive Antenna Selection System for MIMO-NOMA with Energy Harvesting," In *IEEE Systems Journal,* vol. 16, no. 3, pp. 4139-4148, 2022.

[5] S. B. Ajibowu, O. A. Adeleke, and I. A. Ojerinde, "Buffer Aided Relay Selection Technique in a Cooperative Communication Network," *Nigerian Journal of Technological Development,* vol. 19, no. 4, pp. 354-360, 2022.

[6] A. A. Nasir, X. Zhou, S. Durrani, and R. A. Kennedy, "Wireless Powered Relays in Cooperative Communications: Time-Switching Relaying Protocols and Throughput Analysis," *IEEE Transactions on Communications,* vol. 63, no. 5, pp. 1607-1622, 2015.

[7] Y. Liu, Z. Ding, M. Elkacshlan, and H. V. Poor, "Cooperative Non-Orthogonal Multiple Access with Simultaneous Wireless Information and Power Transfer," *IEEE Journal on Selected Areas in Communications,* vol. 34, no. 4, pp. 938-953, 2016.

[8] T. N. Do and A. Beongku, "Optimum sum-throughput analysis for downlink cooperative SWIPT NOMA systems," *2nd International Conference on Recent Advances in Signal Processing, Telecommunications & Computing (SigTelCom),* pp. 85-90, 2018.

[9] Y. Liu, H. Ding, J. Shen, R. Xiao, and J. Yang, "Outage Performance Analysis for SWIPT-based Cooperative Non-Orthogonal Multiple Access Systems," *IEEE Communications Letters,* vol. 23, no. 9, pp. 1501-1505, 2019.

[10] H. Q. Tran, C. V. Phan, and Q. T. Vien, "Power Splitting versus Time Switching based Cooperative Relaying Protocols for SWIPT in NOMA System," *Phys. Commun*. 41, 2020.

[11] O. Alamu, T. O. Olwal, and K. Djouani, "Cooperative NOMA Networks with Simultaneous Wireless Information and Power Transfer: An Overview and Outlook," *Alexandria Engineering Journal,* vol. 71, pp. 413-438, 2023.

[12] V. Aswathi, and A. V. Babu, "Full/Half Duplex Cooperative Relaying NOMA Network under Power Splitting Based SWIPT: Performance Analysis and Optimization," *Phys. Commun.* vol. 46, no. 5, 2021.

[13] T. L. Nguyen, D. H. Ha, P. T. Tin, and N. V. Vinh, "SWIPT-Based Non-Orthogonal Multiple Access under Arbitrary Nakagami-m Fading with Direct links," *Journal of Computer Networks and Communication,* 4, pp. 1-7, 2021.

[14] H. Q. Tran, C. V. Phan, and Q. T. Vien, "Performance Analysis of Power-Splitting Relaying Protocol in SWIPT Based Cooperative NOMA Systems," *EURASIP J. Wireless Commun. Network,* 1, pp. 1-26, 2021.

[15] S. Li, T. Jia, H. Yang, R. Gao, and Q. Yang, "SWIPT Cooperative Protocol for Improving the Communication Quality of Cell-Edge Users in NOMA Networks and its Performance Analysis," *Electronics,* vol. 12, no. 27, pp. 35-83, 2023.

[16] A. Ahmad, W. Z. Fayez, and M. A. Mohammed, "Best Sum-Throughput Evaluation of Cooperative Downlink Transmission Non-Orthogonal Multiple Access System," *International Journal of Electrical and Computer Engineering,* vol. 14, no. 1, pp. 509-519, 2024.

[17] A. Baranwal, S. Sharma, S. D. Roy, and S. Kundu, "On the Performance of a full-duplex SWIPT-enabled Cooperative NOMA network," *Wireless Network,* vol. 30**,** no. 3, pp. 1643-1656, 2024.

[18] S. Parida, P. Kumar, and S. Das, "Performance of SWIPT-Assisted CNOMA System with P-CSI User Selection under Nakagami-m Fading," *Transactions on Emerging Telecommunication Technologies,* vol. 36, no. 1, pp. 1-10, 2024.

[19] C. Song, Y. Wang, Y. Zhou, Y. Ma, E. Li, and K. Hu, "Performance Analysis of Shared Relay CR-NOMA Network based on SWIPT", *EURASIP Journal of Wireless Communications and Networking*. vol. 2024, no. 70, 2024.

[20] M. Liaqat, K.A. Noordin, T.A Latef, K. Dimyati, T. Younas, F. Qamal, and Z. Ding, "Performance Evaluation of Multiple Relay SWIPT-enabled cooperative NOMA Network in the presence of Interference", *Wireless Networks*. vol. 30, no. 4, pp. 2381-2394, 2024.

[21] A. A. Khan, P. M. Thirunavakkarasu, and N. Waqas, "Outage and Throughput Analysis of Cooperative Non-Orthogonal Multiple Access based SWIPT Cognitive Relay Network," *International Journal of Technology,* vol. 16, no. 1, pp. 176-185, 2025.

[22] M. Ashraf, J.W. Jang, J.K. Han, and K.G. Lee "Capacity Maximizing Adaptive Power Splitting Protocol for Cooperative Energy Harvesting Communication System, "Journal of Latex Class Files, vol. 13, no. 9,

[23] Y. Ye, Y. Li, D. Wang, F. Zhou, R.Q. Hu, H. Zhang "Optimal Transmission schemes for DF Relaying Networks using SWIPT". IEEE Transactions on Vehicular Technology, 2018.